

## Mathematical Modelling of Hydromagnetic Convection from a Rotating Sphere with Impulsive Motion and Buoyancy Effects\*

O. Anwar Bég<sup>1</sup>, H.S. Takhar<sup>2</sup>, G. Nath<sup>3</sup>, A.J. Chamkha<sup>4</sup>

<sup>1</sup>Leeds College of Building, Leeds Metropolitan University, North Street, Leeds, LS2 7QT, UK  
obeg@lcb.ac.uk; docoabeg@hotmail.com

<sup>2</sup>Engineering Department, Manchester Metropolitan University, Oxford Rd., Manchester, M5, UK  
h.s.takhar@mmu.ac.uk

<sup>3</sup>Mathematics Department, Indian Institute of Science, Bangalore, 560 012, India

<sup>4</sup>Manufacturing Engineering Department, Public Authority for Applied Education and Training  
Shuweikh, 70654 Kuwait, P.O. Box 42325  
chamkha@paaet.edu.kw

**Received:** 24.02.2006   **Revised:** 15.05.2006   **Published online:** 01.09.2006

**Abstract.** The convective heat transfer on a rotating sphere in the presence of magnetic field, buoyancy forces and impulsive motion is examined theoretically and numerically in this paper. We apply a boundary layer model comprising the balance equations for  $x$  and  $y$  direction translational momentum and heat transfer, and solve these coupled non-linear partial differential equations using Blottner's finite-difference method [1]. The numerical solutions are benchmarked with the earlier study by Lee [2] on laminar boundary layer flow over rotating bodies in forced flow and found to be in excellent agreement. The effects of magnetic field, buoyancy parameter, Prandtl number and thermal conductivity parameter on translational velocities and temperature and other variables (shear stress etc) are presented graphically and discussed at length. The problem finds applications in chemical engineering technologies, aerodynamics and planetary astrophysics.

**Keywords:** hydromagnetic, convection, rotation, Prandtl number, chemical engineering devices, industrial aerodynamics, impulsive motion, numerical, finite difference, Blottner method.

---

\*Dedicated to the memory of the late Professor E. E. Zukoski (1927–1997), formerly Professor of Jet Propulsion, Combustion Laboratories, California Institute of Technology, USA, for his encouragement with hydromagnetic fluid mechanics and its applications in aerodynamics.

## 1 Introduction

The topic of convection heat transfer from rotating bodies has received considerable attention over the past several decades. Studies were conducted by Takhar and Whitelaw [3] who used asymptotic analysis to investigate the higher order heat transfer from a rotating sphere. Lee *et al.* [2] studied the laminar boundary layer flow over rotating bodies in forced convection conditions. Surma Devi *et al.* [4] examined the transient convection flows on a rotating axisymmetric body. The subject of magnetohydrodynamics (MHD) has also developed in many directions and industry has exploited the use of magnetic fields in controlling a range of fluid and thermal processes. Many studies of the influence of magnetism on electrically-conducting flows have been reported with a plethora of other physical phenomena. Poots [5] studied analytically the laminar natural convection magneto-hydrodynamic flows between parallel plane surfaces and also through a horizontal circular tube incorporating viscous and Joule electrical dissipation effects as well as internal energy generation. He showed that velocities and heat transfer rates were reduced by magnetic field. Soundalgekar and Takhar [6] investigated the MHD oscillatory flow past a flat plate, showing numerically that for flat plate flows magnetic field depresses heat transfer rates. Takhar and Pop [7] examined the magneto-convection flow from a wedge at high Prandtl numbers. Niranjana *et al.* [8] examined the MHD free convection in a horizontal channel with the effects of Hall currents. Takhar *et al.* [9] studied the unsteady magnetohydrodynamic flow of a dusty viscous liquid in a revolving channel in the presence of Hall currents. Bég *et al.* [10] studied numerically the effects of magnetic field on non-Darcy viscoelastic convection in porous media. Takhar *et al.* [11] also investigated the effects of electromagnetic field on Newtonian convection in non-Darcy porous media. In the present problem we shall study the effects of magnetic field, buoyancy parameter, thermal conductivity and Prandtl number on impulsive thermal convection on a rotating sphere.

## 2 Flow model

Let us consider the unsteady laminar boundary layer flow of a viscous electrically-conducting fluid in the vicinity of the front stagnation point of a rotating sphere

in the presence of a magnetic field and a buoyancy force. Prior to the time  $t = 0$ , the sphere is stationary and immersed in an ambient fluid with surface temperature  $T_\infty$  which is the same as that of the surrounding fluid. At time  $t = 0$ , an impulsive motion is imparted to the ambient fluid and the sphere is suddenly rotated with constant angular velocity  $\Omega$ . At the same time the surface temperature of the sphere is suddenly increased to  $T_w$  ( $T_w > T_\infty$ ). A constant magnetic field  $B$  is applied in the  $z$  direction. It is assumed that the magnetic Reynolds number  $R_m = \mu_0 RVL \ll 1$ , where  $\mu_0$  is the magnetic permeability,  $R$  is the radius of the sphere,  $L$  and  $V$  are the characteristic length and velocity respectively. Under these conditions it is possible to neglect the effect of the induced magnetic field as compared with the applied magnetic field. The wall and the free stream temperatures are taken as constant. The viscous dissipation terms, Ohmic heating and surface curvature are neglected in the vicinity of the stagnation point. The hydrodynamic flow field is assumed to be axisymmetric and the fluid possesses constant thermophysical properties with the exception of those caused by density changes which generate the buoyancy force, under the Boussinesq approximation. It is also assumed that the effect of the buoyancy-induced streamwise pressure gradient terms on the flow and temperature fields is negligible. In the vicinity of the front stagnation point,  $\gamma$  and  $d\gamma/dx$  are of the order of unity, where  $\gamma$  is a function of  $x$  and designates the radius of a section normal to the axis of the sphere and is assumed large in comparison to the boundary layer thickness. Under these thermophysical assumptions, the boundary layer equations, based on the conservation of mass, momentum and energy, describing the flow regime, can be cast as follows:

Continuity:

$$\partial(uv)/\partial x + \partial(vv)/\partial z = 0, \quad (1)$$

$x$ -direction Momentum:

$$\begin{aligned} \partial u/\partial t + u \partial u/\partial x + w \partial u/\partial z - v^2/x \\ = u_e du_e/dx + \nu \partial^2 u/\partial z^2 + g\beta(T - T_\infty)[x/R] - [\sigma B^2/\rho](u - u_e), \end{aligned} \quad (2)$$

$y$ - direction Momentum:

$$\partial v/\partial t + u \partial v/\partial x + w \partial v/\partial z + uv/x = \nu \partial^2 v/\partial z^2 - [\sigma B^2/\rho]v, \quad (3)$$

Energy (Heat):

$$\partial T/\partial t + u \partial T/\partial x + w \partial T/\partial z = \alpha_1 \partial^2 T/\partial z^2. \quad (4)$$

The *initial* conditions for the flow regime are:

$$u(x, z, t) = v(x, z, t) = w(x, z, t) = 0, \quad T(x, z, t) = T_\infty \quad \text{for } t < 0. \quad (5)$$

The *boundary* conditions for  $t \geq 0$  are:

$$\begin{aligned} u(x, 0, t) = 0, \quad v(x, 0, t) = \Omega x, \quad w(x, 0, t) = 0, \quad T(x, 0, t) = T_w, \\ u(x, \infty, t) = u_e(x), \quad v(x, \infty, t) = 0, \quad T(x, \infty, t) = T_\infty, \end{aligned} \quad (6)$$

where  $x$  denotes distance along a meridian of the sphere from the forward stagnation point,  $y$  is the distance in the direction of rotation,  $z$  is the distance normal to the surface;  $u, v$  and  $w$  are the velocity components along the  $x, y$  and  $z$  directions respectively,  $\sigma$  is the electrical conductivity of the fluid,  $T$  is the temperature,  $t$  denotes time,  $B$  is magnetic field,  $\rho$  is the fluid density,  $\nu$  is the kinematic viscosity,  $\Omega$  is the angular velocity of the sphere,  $g'$  denotes gravitational acceleration,  $\alpha_1$  is the thermal diffusivity,  $\beta$  is the coefficient of thermal expansion. The subscripts  $e, w$  and  $\infty$  denote conditions at the edge of the boundary layer, on the surface and in the free stream, respectively.

### 3 Transformation of equations

It is possible and beneficial from a numerical solution viewpoint, to convert the partial differential equations of transport (1)–(4) and boundary conditions (5) and (6) with *three* independent variables ( $t, x, z$ ) to dimensionless partial differential equations with *two* independent variables ( $\xi, \eta$ ) by applying the following transformations:

$$t^* = \alpha t, \quad a > 0, \quad (7)$$

$$\xi = 1 - \exp(-t^*), \quad (8)$$

$$\eta = (2a/\nu)^{1/2} \xi^{-1/2} z, \quad (9)$$

$$u_e = ax, \quad (10)$$

$$v_w = \Omega x, \quad (11)$$

$$u(x, z, t) = ax \partial f(\xi, \eta) / \partial \eta, \quad (12)$$

$$v(x, z, t) = \Omega x s(\xi, \eta), \quad (13)$$

$$w(x, z, t) = -(2a\nu)^{1/2} \xi^{1/2} f(\xi, \eta), \quad (14)$$

$$T(x, z, t) = T_\infty + (T_w - T_\infty) g(\xi, \eta), \quad (15)$$

$$\lambda = (\Omega/a)^2, \quad (16)$$

$$Pr = \nu/\alpha_1, \quad (17)$$

$$a = du_e/dx, \quad (18)$$

$$M = \sigma B^2 / \rho a, \quad (19)$$

$$\alpha = Gr_R / Re_R^2, \quad (20)$$

$$Gr_R = g' \beta (T_w - T_\infty) R^3 / \nu^2, \quad (21)$$

$$Re_R = aR^2 / \nu. \quad (22)$$

The governing equations are therefore transformed to the following system of collectively seventh order partial differential equations with reference to a  $(\xi, \eta)$  coordinate system.

*x*-direction Momentum:

$$\begin{aligned} \frac{\partial^3 f}{\partial \eta^3} + \frac{\eta}{4}(1-\xi) \frac{\partial^2 f}{\partial \eta^2} + \xi f \frac{\partial^2 f}{\partial \eta^2} - \frac{1}{2} \xi \left[ \left( \frac{\partial f}{\partial \eta} \right)^2 - 1 - \lambda s^2 \right] \\ + \frac{\xi}{2} M \left[ 1 - \left( \frac{\partial f}{\partial \eta} \right) \right] + \frac{1}{2} \xi \alpha g = \frac{1}{2} \xi (1-\xi) \left[ \frac{\partial^2 f}{\partial \xi \partial \eta} \right], \end{aligned} \quad (23)$$

*y*-direction Momentum:

$$\frac{\partial^2 s}{\partial \eta^2} + \frac{\eta}{4}(1-\xi) \frac{\partial s}{\partial \eta} + \xi \left[ f \frac{\partial s}{\partial \eta} - s \frac{\partial f}{\partial \eta} \right] - \frac{\xi}{2} M s = \frac{\xi}{2} (1-\xi) \left[ \frac{\partial s}{\partial \xi} \right], \quad (24)$$

Energy (Heat):

$$\frac{1}{Pr} \frac{\partial^2 g}{\partial \eta^2} + \frac{\eta}{4}(1-\xi) \frac{\partial g}{\partial \eta} + \xi \left[ f \frac{\partial g}{\partial \eta} \right] = \frac{\xi}{2} \xi (1-\xi) \left[ \frac{\partial g}{\partial \xi} \right], \quad (25)$$

Boundary Conditions:

$$f(\xi, 0) = \frac{\partial f}{\partial \eta}(\xi, 0) = 0, \quad s(\xi, 0) = g(\xi, 0) = 1, \quad (26)$$

$$\frac{\partial f}{\partial \xi}(\xi, \infty) = 1, \quad s(\xi, \infty) = g(\xi, \infty) = 0, \quad (27)$$

where  $t^*$  and  $\xi$  are the dimensionless time,  $\eta$  is the transformed variable in the  $z$  direction,  $\partial f/\partial\eta$  and  $s$  denote the dimensionless velocity components along the  $x$  and  $y$  directions, respectively,  $g$  is the dimensionless temperature function,  $M$  is the Hartmann hydromagnetic number (the magnetic field acts in the  $z$  direction),  $\lambda$  is a rotational parameter (identical to the parameter  $B$  in the study by Lee *et al.* [2]),  $a$  is the velocity gradient at the edge of the boundary layer,  $Gr_R$  is the Grashof free convection number,  $Re_R$  is the Reynolds number,  $\alpha$  is the buoyancy parameter,  $Pr$  denotes Prandtl number. There are four key thermophysical parameters dictating the flow regime –  $M$ ,  $\alpha$ ,  $Pr$  and  $\lambda$ .

#### 4 Numerical solution by blottner difference scheme

The governing equations amount to a *seventh* order set of nonlinear, coupled partial differential equations with seven corresponding boundary conditions. The Blottner method has been used in a wide range of thermoconvection and fluid mechanics problems. Chamkha [12] studied the combined natural convection heat and mass transfer from various geometries in a porous medium using the Blottner scheme. Details of the numerics are to be found in this reference. We shall therefore not relate these aspects here. *For brevity we denoted  $\partial/\partial\eta$  by the superscript ( $'$ ) and this format is followed in the table and graphs plotted.*

#### 5 Results and discussion

We have computed profiles for the special case of  $\xi = 1$ ,  $\alpha = M = 0$  i.e. zero buoyancy and no magnetic field i.e. purely hydrodynamic heat transfer, respectively. The simplified equations correspond exactly to the earlier equations solved by Lee *et al.* [2], viz:

*x*-Momentum:

$$\frac{\partial^3 f}{\partial\eta^3} + f \frac{\partial^2 f}{\partial\eta^2} + \frac{1}{2} - \frac{1}{2} \left( \frac{\partial f}{\partial\eta} \right)^2 + \frac{1}{2} \lambda s^2 = 0, \quad (28)$$

*y*-Momentum:

$$\frac{\partial^2 s}{\partial\eta^2} + f \frac{\partial s}{\partial\eta} - s \frac{\partial f}{\partial\eta} = 0, \quad (29)$$

Thermal Energy (Heat):

$$\frac{\partial^2 g}{\partial \eta^2} + Pr f \frac{\partial g}{\partial \eta} = 0. \quad (30)$$

The computations have been tabulated at  $\xi = 1$  for three combinations of the Prandtl number and the thermal conductivity parameter. The results of Lee *et al.* [2] for  $x$ -direction shear stress  $f''(\xi, 0)$ ,  $y$ -direction shear stress  $s'(\xi, 0)$  and surface heat transfer rate  $g'(\xi, 0)$  are therefore tabulated for  $Pr = 1, 10$  and  $100$ . The case in Lee *et al.*'s model [2] for  $\xi = 0$  and  $\Lambda = 0.5$  reduces their equations to the set given above i.e. (28), (29) and (30). In the top section of Table 1, we observe that for all values of rotation parameter  $\lambda$  (i.e. 1, 4, 10) with  $Pr = 1.0$ , the values for  $f''(\xi, 0)$ ,  $s'(\xi, 0)$  and  $g'(\xi, 0)$  are identical to three decimal places. Lee *et al.* [2] used a fourth order Runge Kutta numerical method to generate solutions to equations (28), (29) and (30) subject to appropriate boundary conditions. We have in addition plotted the  $f''(\xi, 0)$ ,  $s'(\xi, 0)$  and  $g'(\xi, 0)$  distributions for the special case of  $M = \alpha = 0$  at  $\xi = 1$  for Prandtl numbers ( $Pr$ ) with values of 10 and 100, for all three cases of the rotational parameter  $\lambda = 1, 4, 10$ . For the case of  $Pr = 1.0$  (saturated water at 440 Kelvins – see Incropera and De Witt [13] as  $\lambda$  is increased from 1 through 4 to 10, the  $x$ -direction shear stress  $f''(\xi, 0)$  increases in magnitude since the flow becomes more vigorous and accelerates with greater rotation. This increases the shear stress at the surface of the sphere. Similarly

Table 1. Comparison of the results ( $f''(\xi, 0), s'(\xi, 0), g'(\xi, 0)$ ) with those of Lee *et al.* [2] for  $m = \alpha = 0$  at  $\xi = 1$

$Pr$	$\lambda$	Lee <i>et al.</i> [2]			Present results		
		$f''(\xi, 0)$	$s'(\xi, 0)$	$g'(\xi, 0)$	$f''(\xi, 0)$	$s'(\xi, 0)$	$g'(\xi, 0)$
1	1	1.1129	-0.7849	0.5536	1.11292	-0.78489	0.55361
	4	1.6233	-0.8463	0.5897	1.62316	-0.84639	0.58973
	10	2.5216	-0.9362	0.6432	2.52141	-0.93624	0.64324
10	1	–	–	1.2911	1.11292	-0.78488	1.29095
	4	–	–	1.4180	1.62318	-0.84636	1.41776
	10	–	–	1.6003	2.52139	-0.93624	1.60004
100	1	–	–	2.8796	1.11291	-0.78488	2.87944
	4	–	–	3.2172	1.62316	-0.84636	3.21673
	10	–	–	3.6860	2.52143	-0.93622	3.68484

the magnitude of the  $y$ -direction shear stress  $| -s'(\xi, 0) |$  and the surface heat transfer rate  $-g'(\xi, 0)$  is also enhanced with rising  $\lambda$  parameter. Similar trends are observed for the case of  $Pr = 10$  (which corresponds to saturated water at 440 Kelvins) and for  $Pr = 100$  (which corresponds to Ethylene Glycol fluid at 310 Kelvins and also to unused engine oils at 420 Kelvins). We note that for more viscous fluids e.g. oils, the Prandtl number is significantly higher and much less energy is therefore transferred by diffusion as compared with momentum transfer.

For the full mathematical model, equations (23), (24) and (25) with boundary conditions (26) and (27), we study initially the effects of magnetism  $M$  on the flow regime. Fig. 1 illustrates the  $x$ -direction shear stress  $f''(\xi, 0)$  versus dimensionless time  $\xi$  for a fixed  $Pr = 0.7$  (i.e. air at 350 Kelvins or Hydrogen gas at 350 Kelvins),  $\lambda = 1$ ,  $\alpha = 1$ . As  $M$  rises we observe that the  $x$ -direction shear stress is enhanced. This trend agrees with a similar behaviour in hydromagnetic flow on a spinning disk studied by Takhar *et al.* [14]. Fig. 2 shows that the  $y$ -direction shear stress  $-s'(\xi, 0)$  is also boosted in value by increasing magnetic parameter  $M$  from 0 to 5, as again this stress is not affected adversely by the magnetic field. The case for  $M = 0$  clearly corresponds to purely thermal convection flow and in this case the  $y$ -direction shear stress is a minimum. We have used in all Figs. 1 to 12 a dimensionless time abscissa range of 1.0. In both Figs. 1 and 2, the maximum values for  $f''(\xi, 0)$  and  $-s'(\xi, 0)$  are at a maximum where  $x = 1.0$  i.e. at the end of the dimensionless time range. Hence shear stresses are increasing simultane-

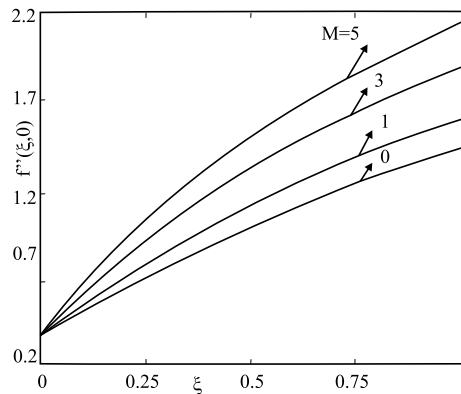


Fig. 1. Variation of  $f''(\xi, 0)$  with  $\xi$  for  $\lambda = \alpha = 1$  and  $Pr = 0.7$ .

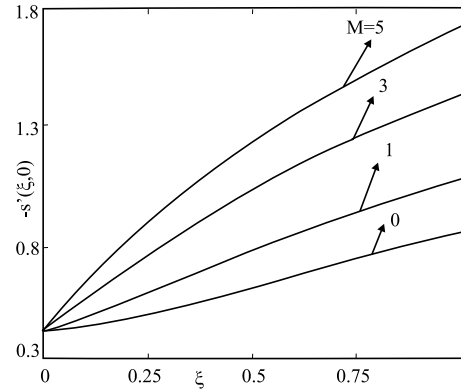


Fig. 2. Variation of  $-s'(\xi, 0)$  with  $\xi$  for  $\lambda = \alpha = 1$  and  $Pr = 0.7$ .

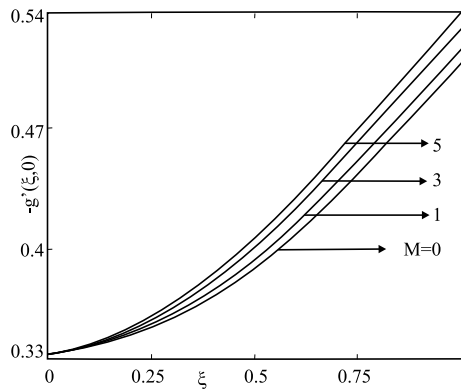


Fig. 3. Variation of  $-g'(\xi, 0)$  with  $\xi$  for  $\lambda = \alpha = 1$  and  $Pr = 0.7$ .

ously with magnetic field and also time. The Prandtl number for Fig. 2 is again 0.7 and  $\lambda$  and  $\alpha$  both have unity values. Fig. 3 shows the variation of non-dimensional surface heat transfer i.e. temperature gradient  $-g'(\xi, 0)$  with  $x$  for various  $M$  values. Again we observe rise in  $-g'(\xi, 0)$  magnitude as  $M$  is increased from 0 to 5. The increase however is not as substantial as for  $f''(\xi, 0)$  and  $-s'(\xi, 0)$ . This is explained by the fact that the magnetic parameter  $M$  appears explicitly in both  $x$  and  $y$  direction momentum equations (23) and (24) where the magnetic terms are respectively  $0.5 \xi M(1 - f')$  and  $-0.5 \xi M s$  respectively. No magnetic term appears in the thermal energy equation (25) and therefore magnetic field

effects are indirectly applied to the thermal field by first affecting the  $x$ -direction and  $y$  direction momentum fields which via coupled terms then affect the energy equation.

The effects of the buoyancy parameter,  $\alpha$ , on  $x$  direction and  $y$  direction shear stresses and also surface heat transfer i.e.  $f''(\xi, 0)$ ,  $-s'(\xi, 0)$  and  $-g'(\xi, 0)$  respectively versus  $x$  are shown in Figs. 4, 5 and 6. The buoyancy parameter only appears in the transformed  $x$  direction momentum equation (23) in the term  $0.5 \xi \alpha g$ . This term couples this equation to the heat (thermal energy equation (25)) and the flow regime is therefore a natural or mixed convection flow regime

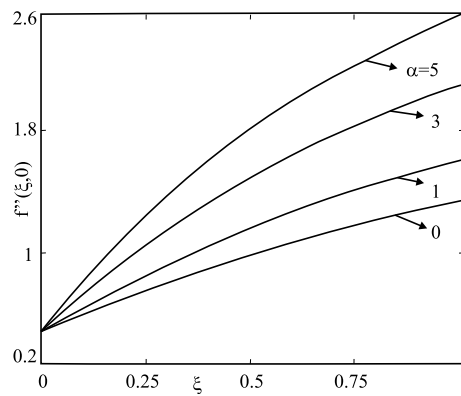


Fig. 4. Variation of  $f''(\xi, 0)$  with  $\xi$  for  $M = \lambda = 1$  and  $Pr = 0.7$ .

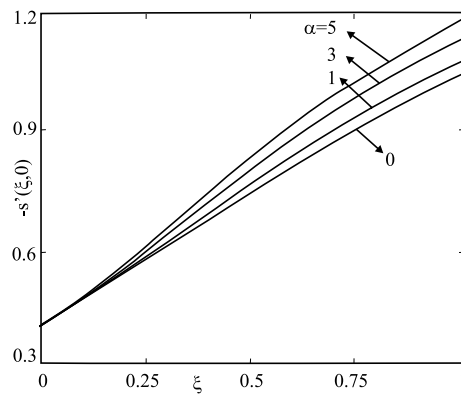


Fig. 5. Variation of  $-s'(\xi, 0)$  with  $\xi$  for  $M = \lambda = 1$  and  $Pr = 0.7$ .

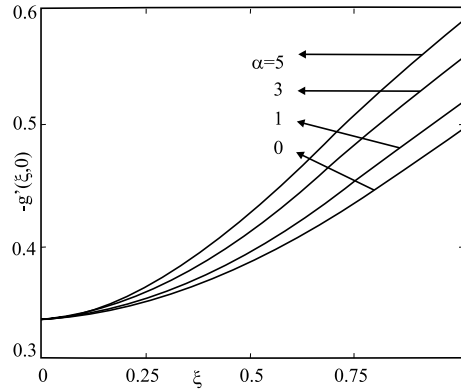


Fig. 6. Variation of  $-g'(\xi, 0)$  with  $\xi$  for  $M = \lambda = 1$  and  $Pr = 0.7$ .

i.e. not forced convection. For forced convection  $\alpha = 0$  and this de-couples the momentum and thermal fields. The coupling of (23) and (25) is valid according to the Boussinesq approximation as discussed by Incropera and De Witt [13]. In Figs. 4, 5 and 6 all plots have been produced for  $M = \lambda = 1$  and  $Pr = 0.7$ . Hence the flow is weakly magnetohydrodynamic with weak rotation as  $\lambda > 0$  and  $M > 0$ . These constitute a laminar magneto-convection flow field.

Fig. 4 shows that  $x$  direction surface shear stress rises considerably as  $\alpha$  rises from 0 to 1. Rising buoyancy factor adds vigour to the flow regime and momentum is also boosted considerably. Consequently the flow is accelerated, velocities and shear stresses are thus elevated. Values are also a maximum for  $\xi = 1$  as buoyancy effects exert greater influence with *time*. A similar trend is observed for the variation of  $-s'(\xi, 0)$  in Fig. 5, i.e.  $y$  direction shear stress increases also with dimensionless time  $\xi$ . The profiles rise more steeply in this case than they do for  $x$  direction shear stress  $f''(\xi, 0)$  and again they peak at a maximum value of  $\xi$  i.e. at the end of the range. Variation of surface heat transfer  $-g'(\xi, 0)$  with  $\xi$  for different  $\alpha$  parameters is plotted in Fig. 6. Once again increasing buoyancy ( $\alpha$ ) elevates the heat transfer rate which rises from a maximum value of about 0.5 for  $\alpha = 0$ , to a value of 0.58 approximately for  $\alpha = 5$  (strong buoyancy).

The effects of rotation parameter  $\lambda$  on  $f''(\xi, 0)$ ,  $-s'(\xi, 0)$  and  $-g'(\xi, 0)$  versus  $\xi$  are plotted in Figs. 7, 8 and 9 respectively. An increase in the rotational parameter substantially boosts the  $\xi$  direction shear stress  $f''(\xi, 0)$  which approximately quadruples in peak value from  $\lambda = 1$  and  $\lambda = 20$ . The magnetic parameter

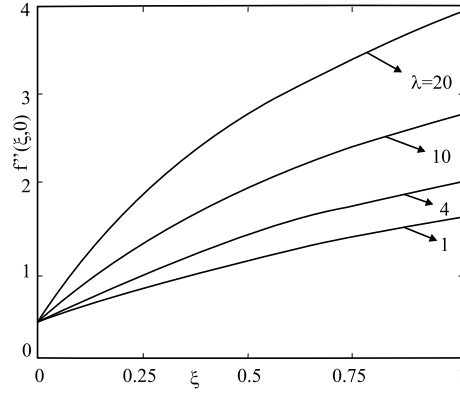


Fig. 7. Variation of  $f''(\xi, 0)$  with  $\xi$  for  $M = \alpha = 1$  and  $Pr = 0.7$ .

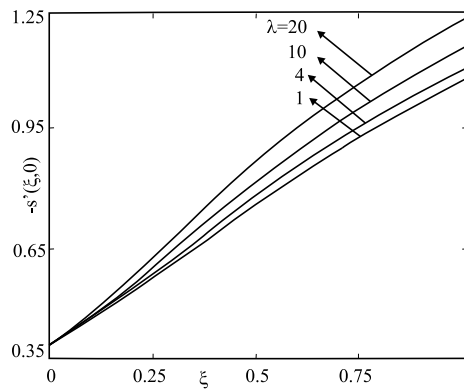


Fig. 8. Variation of  $-s'(\xi, 0)$  with  $\xi$  for  $M = \alpha = 1$  and  $Pr = 0.7$ .

$M$  and buoyancy parameter  $a$  are both equal to 1 and  $Pr$  is 0.7 corresponding to weakly buoyant aerodynamic hydromagnetic convection. The  $y$  direction shear stress (Fig. 8) increases less noticeably with a rise in  $\lambda$ . Increasing  $\lambda$  from 1 to 20 only boosts the  $-s'(\xi, 0)$  magnitude from 1.1 approximately to about 1.24 at the end of the  $\xi$  range. The lesser effects are explained by the fact that  $\lambda$  does not occur explicitly in the  $y$  direction momentum equation (24). It only occurs in the  $x$  direction momentum equation where it appears as  $0.5\xi\lambda s^2$ . This term serves to strongly couple the  $x$  direction and  $y$  direction momentum equations as  $s$  is present in this term. The  $\lambda$  parameter therefore indirectly affects the  $y$  direction velocity,  $s$ , and  $y$  direction shear stress,  $-s'(\xi, 0)$ , via the  $x$  direction momentum

equation.

Fig. 9 depicts the distribution of local surface heat transfer  $-g'(\xi, 0)$  with  $\xi$  for various  $\lambda$  values. As with the  $y$  direction momentum equation (24), the rotational parameter  $\lambda$  does not appear in the heat equation (25) but dimensionless temperature  $g$  is coupled with stream function  $f$  via the buoyancy term  $0.5 \xi \alpha g$  which occurs in the  $x$  direction momentum equation (23). Consequently  $\lambda$  affects the  $x$  direction flow equation and these effects are transferred through to the heat equation via the  $\xi f g'$  term in this equation (25). The plots for  $\lambda = 1, 4, 10$  and  $20$  are less different therefore and  $-g'(\xi, 0)$  increases from a peak value of about 0.5 for  $\lambda = 1$  to about 0.6 for  $\lambda = 20$  i.e. the difference (increase) is less than 25 %.

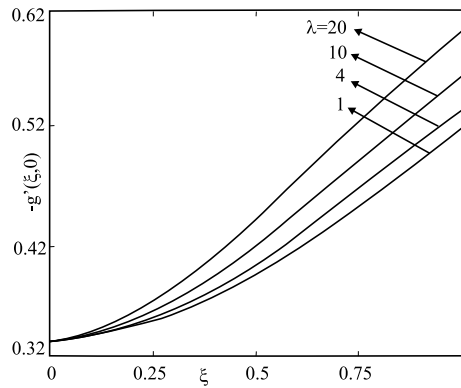


Fig. 9. Variation of  $-g'(\xi, 0)$  with  $\xi$  for  $M = \alpha = 1$  and  $Pr = 0.7$ .

Figs. 10 to 12 illustrate the variation of  $f''(\xi, 0)$ ,  $-s'(\xi, 0)$  and  $-g'(\xi, 0)$  versus  $\xi$  for various Prandtl numbers ( $Pr$ ). In all three plots  $\lambda$  is fixed at 1 as is  $\alpha$ .  $Pr = 0.7$  corresponds to air at 350 Kelvins but rising  $Pr$  corresponds to saturated water at 330 Kelvins ( $Pr = 3$ ) and  $Pr = 7$  is approximately the value for saturated water at 290 Kelvins  $Pr = 15$  implies certain oils and lubricants. Fig. 10 shows that  $x$  direction surface shear stress  $f''(\xi, 0)$  is decreased by increasing  $Pr$  from 0.7 to 15.  $Pr$  is defined as the ratio of momentum and thermal diffusivities. For higher  $Pr$  fluids the flow regime is decelerated (greater viscosities) and this decreases shear stresses at the surface of the sphere. A decrease in  $y$  direction shear stress  $-s'(\xi, 0)$  is seen in Fig. 11, as  $Pr$  rises from 0.7 to 15. We note the effect of  $Pr$  on both  $f''(\xi, 0)$  and  $-s'(\xi, 0)$  as  $Pr$  only appears in the heat equa-

tion, but since  $f$  also appears in the heat equation (25) it is affected more strongly than  $s$ , by  $Pr$ . The effects on  $-s'(\xi, 0)$  are indirectly caused by the coupling of  $f$  and  $\xi$  with the  $y$  direction momentum equation. There is no  $g$  term in equation (24) or  $s$  term in equation (25) i.e. they are not coupled via the  $y$  direction velocity or temperature fields.

As expected Fig. 12 shows a dramatic rise in  $-g'(\xi, 0)$  from  $Pr = 0.7$  to  $Pr = 15$  as  $Pr$  boosts the convection heat transfer and increases the rate of energy (thermal) transferred from the surface of the sphere to the engulfing fluid.  $M = \lambda = \alpha = 1$  for this flow scenario which physically implies a weak hydromagnetic field, slow rotation and weak buoyancy forces. Temperatures would also fall with

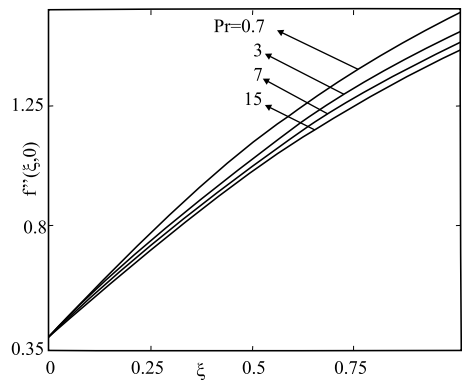


Fig. 10. Variation of  $f''(\xi, 0)$  with  $\xi$  for  $M = \lambda = \alpha = 1$ .

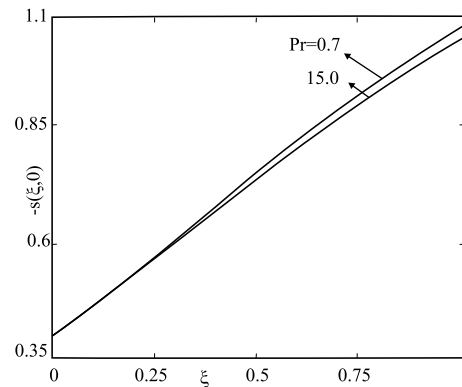


Fig. 11. Variation of  $-s'(\xi, 0)$  with  $\xi$  for  $M = \lambda = \alpha = 1$ .

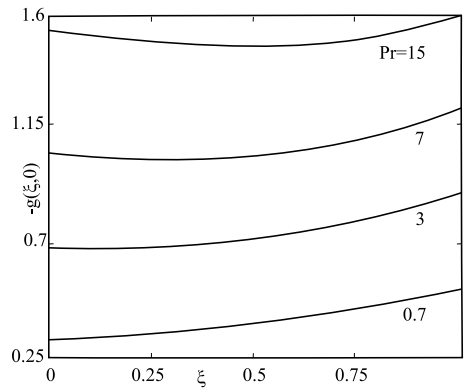


Fig. 12. Variation of  $-g'(\xi, 0)$  with  $\xi$  for  $M = \lambda = \alpha = 1$ .

rising  $Pr$  but these have not been plotted against  $\xi$ . These results concur with the earlier analysis of Takhar *et al.* [11].

Figs. 13 to 15 plot the non-dimensional  $x$  direction velocity  $f'(\eta)$ ,  $y$  direction velocity  $s(\eta)$  and temperature  $g(\eta)$  with  $\eta$  coordinate for various values of  $\xi$  i.e. dimensionless time. As expected  $f'(\eta)$  rises with  $\xi$  increasing from 0 to 0.5 to 1.0 since the fluid is accelerated with time.  $M = \alpha = \lambda = 1$  and  $Pr = 0.7$  for all plots 14 to 16.  $y$  direction velocity is depressed (Fig. 15) with rising  $\xi$  i.e. maximum  $y$  direction velocities occur at the start of the impulsive motion ( $\xi = 0.0$ ). The effects of this impulse are reduced with time and exhibited by a substantial depression in  $y$  direction velocity. A similar trend is observed

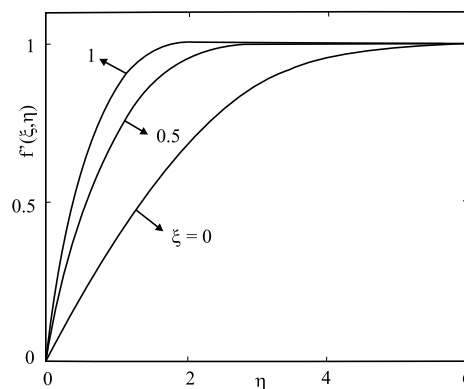


Fig. 13. Velocity profile  $f'(\xi, \eta)$  for  $M = \lambda = \alpha = 1$  and  $Pr = 0.7$ .

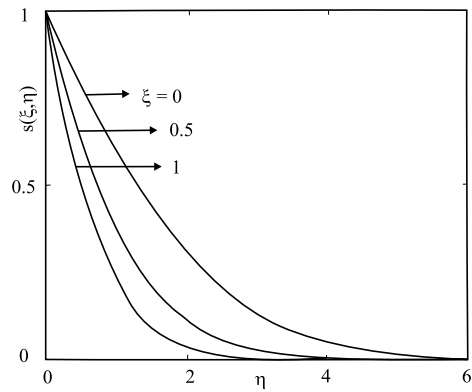


Fig. 14. Velocity profile  $s(\xi, \eta)$  for  $M = \lambda = \alpha = 1$  and  $Pr = 0.7$ .

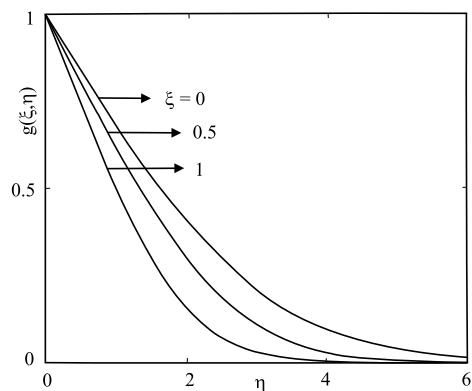


Fig. 15. Velocity profile  $g(\xi, \eta)$  for  $M = \lambda = \alpha = 1$  and  $Pr = 0.7$ .

for Fig. 15 where dimensionless temperature  $g(\eta)$  is plotted against  $\eta$ . In all three plots 13, 14 and 15, we have utilised an  $\eta$  range of  $[2]$  as this allows convergence with a high degree of accuracy for the Blottner numerical finite difference method. Temperatures are depressed as time proceeds i.e. the  $\xi = 1$  profiles are significantly lower than the  $\xi = 0$  profiles.

## 6 Conclusions

A mathematical model has been derived for the rotating heat transfer from a spherical body in the presence of strong magnetic field and impulsive and buoyancy

effects. A benchmarked numerical solution has been obtained to the transformed boundary layer equations using a robust finite difference scheme introduced by Blottner [1] for aerodynamics simulations. The numerical code has been verified by comparison with previous computations by Lee *et al.* for the non-magnetic case. Our computations indicate:

1. Increasing magnetic field ( $M$ ) enhances magnitudes of the  $x$ -direction shear stress ( $f''(\xi, 0)$ ) is enhanced and also the  $y$ -direction shear stress  $-s'(\xi, 0)$  is also boosted in value by increasing magnetic parameter  $M$  from 0 to 5.

2. Non-dimensional surface heat transfer i.e. temperature gradient  $-g'(\xi, 0)$  is also increased with a rise in magnetic field parameter,  $M$ . The increase however is not as substantial as for  $f''(\xi, 0)$  and  $-s'(\xi, 0)$  as convection is only affected indirectly by the influence of the magnetic field on the flow fields.

3. Rising buoyancy factor ( $\alpha$ ) accelerates the flow and increases both  $x$ -direction shear stress ( $f''(\xi, 0)$ ), and the  $y$ -direction shear stress ( $-s'(\xi, 0)$ ). The profiles however ascend more steeply in the latter case than they do for  $x$  direction shear stress,  $f''(\xi, 0)$ . This can have significant influence in chemical treatment processes involving very high rotational velocities as described by Lee *et al.* [2].

4. Increasing buoyancy ( $\alpha$ ) elevates the heat transfer rate i.e.  $-g'(\xi, 0)$ , which is beneficial in rotational process control in chemical engineering systems as described by Takhar and Whitelaw [3].

5. Rising rotational parameter ( $\lambda$ ) greatly enhances the  $x$  direction shear stress  $f''(\xi, 0)$  and also increases the  $y$ -direction shear stress i.e.  $-s'(\xi, 0)$  magnitude, although to a much lesser extent. Primary flow is therefore considerably accelerated by the increase in rotational velocity whereas  $\lambda$  (rotation parameter) only weakly affects the secondary flow regime.

6. The non-dimensional surface heat transfer rate,  $-g'(\xi, 0)$  is positively affected by a rise in rotation parameter ( $\lambda$ ) but to a much lesser extent than the flow fields.

7. Increasing Prandtl number ( $Pr$ ) strongly decreases the  $x$ -direction surface shear stress  $f''(\xi, 0)$  and also the  $y$ -direction shear stress  $-s'(\xi, 0)$ .

8. Rising  $Pr$  largely increases the non-dimensional surface heat transfer rate,  $-g'(\xi, 0)$  since larger  $Pr$  values augment convection heat transfer and boost heat transferred from the surface of the sphere to the engulfing fluid. Therefore

in industrial applications higher  $Pr$  fluids are more effective in enhancing heat transfer to ambient fluids with the converse apparent for lower  $Pr$  values. Such results concur also with the case for a rotating flat plate as described by Bég *et al.* [15].

The present study is currently being extended to examine the heat transfer and flow field characteristics of more complex non-Newtonian fluids, the results of which will be communicated in future research (Bég *et al.* [16, 17]).

## References

1. F. G. Blottner, Finite-difference methods of solution of the boundary layer equations, *AIAA Journal*, **8**(2), pp. 193–205, 1970.
2. M. H. Lee, D. R. Jeng, K. J. De Witt, Laminar boundary layer transfer over rotating bodies in forced flow, *ASME J. Heat Transfer*, **100**(3), pp. 496–502, 1978.
3. H. S. Takhar, M. H. Whitlaw, Higher order heat transfer from a rotating sphere, *Acta Mechanica*, **30**(1–2), pp. 101–109, 1978.
4. C. D. Surma Devi, H. S. Takhar, G. Nath, Unsteady free convection boundary layers on a rotating axisymmetric body, *Acta Technica*, **32**, pp. 354–365, 1978.
5. G. Poots, Laminar natural convection flow in magneto-hydrodynamics, *Int. J. Heat and Mass Transfer*, **3**(1), pp. 1–25, 1961.
6. V. M. Soundalgekar, H. S. Takhar, MHD oscillatory flow past a semi-infinite plate, *AIAA Journal*, **15**(4), pp. 457–458, 1977.
7. H. S. Takhar, I. Pop, On MHD heat transfer from a wedge at large Prandtl numbers, *Mechanics Research Communications*, **11**(3), pp. 191–194, 1984.
8. S. S. Niranjana, V. M. Soundalgekar, H. S. Takhar, Free convection effects on MHD horizontal channel flow with Hall currents, *IEEE Transactions on Plasma Science*, **18**(2), pp. 177–183, 1990.
9. H. S. Takhar, P. C. Ram, S. S. Singh, Unsteady MHD flow of a dusty viscous liquid in a rotating channel with Hall currents, *Int. J. Energy Research*, **17**, pp. 69–74, 1993.
10. O. A. Bég, H. S. Takhar, M. Kumari, G. Nath, Computational fluid dynamics modelling of buoyancy-induced viscoelastic flow in a porous medium with magnetic field effects, *Int. J. Applied Mechanics and Engineering*, **6**, pp. 187–210, 2001.

11. H. S. Takhar, A. J. Chamkha, O. A. Bég, Numerical modelling of Darcy-Brinkman-Forscheimmer magneto-hydrodynamic convection flow in a porous medium with transpiration and viscous heating, *Int. J. Fluid Mechanics Research*, **29**(1), pp. 1–26, 2002.
12. A. J. Chamkha, A-R. A. Khaled, O. Al-Hawaj, Simultaneous heat and mass transfer by natural convection from a cone and a wedge in porous media, *J. Porous Media*, **3**(2), pp. 155–164, 2000.
13. F. P. Incropera, D. P. De Witt, *Fundamentals of Heat and Mass Transfer*, 3rd Edition, John Wiley & Sons, 1990.
14. H. S. Takhar, A. K. Singh, G. Nath, Unsteady MHD Flow and heat transfer on a rotating disk in an ambient fluid, *Int. J. Thermal Sciences*, **41**(2), pp. 147–155, 2002.
15. O. A. Bég, H. S. Takhar, G. Nath, O. A. Bég, A. J. Chamkha, R. Majeed, Modeling convection heat transfer in a rotating fluid in a thermally-stratified high-porosity medium: Numerical finite difference solutions, *Int. J. Fluid Mechanics Research*, May, **34**(6), pp. 1–18, 2005.
16. O. A. Bég, H. S. Takhar, N. Baruah, R. Bhargava, Computational simulation of unsteady MHD Flow and Heat transfer on a Rotating Sphere to Oldroyd-B fluids, *Applied Mathematical Modeling J.*, in preparation, 2006.
17. O. A. Bég, H. S. Takhar, N. Baruah, R. Bhargava, Magneto-Micropolar Convection from a rotating sphere with Joule Heating: finite element solutions, *Int. J. Dynamics of Fluids*, in preparation, 2007.
18. A. J. Chamkha, Hydromagnetic natural convection from an isothermal inclined surface adjacent to a thermally stratified porous medium, *Int. J. Engineering Science*, **35**(10–11), pp. 975–986, 1997.